

ChemComm

Accepted Manuscript



This is an *Accepted Manuscript*, which has been through the Royal Society of Chemistry peer review process and has been accepted for publication.

Accepted Manuscripts are published online shortly after acceptance, before technical editing, formatting and proof reading. Using this free service, authors can make their results available to the community, in citable form, before we publish the edited article. We will replace this *Accepted Manuscript* with the edited and formatted *Advance Article* as soon as it is available.

You can find more information about *Accepted Manuscripts* in the [Information for Authors](#).

Please note that technical editing may introduce minor changes to the text and/or graphics, which may alter content. The journal's standard [Terms & Conditions](#) and the [Ethical guidelines](#) still apply. In no event shall the Royal Society of Chemistry be held responsible for any errors or omissions in this *Accepted Manuscript* or any consequences arising from the use of any information it contains.

COMMUNICATION

Sign Inversion of Circularly Polarized Luminescence by Geometry Manipulation of Four Naphthalene Units Introduced to a Tartaric Acid Scaffold

Cite this: DOI: 10.1039/x0xx00000x

Received 00th January 2012,
Accepted 00th January 2012Tomoyuki Amako,^a Kazuki Nakabayashi,^a Tadashi Mori,^{b*} Yoshihisa Inoue,^b Michiya Fujiki,^{c*} and Yoshitane Imai^{a*}

DOI: 10.1039/x0xx00000x

www.rsc.org/

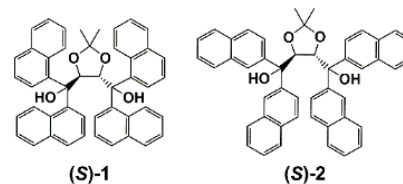
Tethering four 1- versus 2-naphthyls to the same chiral scaffold derived from tartaric acid led to the oppositely signed circularly polarized luminescence (CPL) and circular dichroism (CD) in solution, which not only reveals the decisive role of the spatial arrangement of chromophores/fluorophores in determining the chiroptical behaviors but also provides us with a versatile tool for switching the signs of CPL and CD without using the antipodal scaffold.

Controlling optical properties of organic compounds is essential for the development of novel, advanced, and well-defined functional organic materials. Organic fluorophores, in particular, attract considerable attention in the fields of optoelectronics and photobiological chemistry.¹ Although a wide range of chiral organic fluorophores have been developed, chiral organic fluorophores emitting circularly polarized luminescence (CPL) with high quantum efficiencies are still limited in number.²

The sign inversion of CPL can be achieved typically by attaching the same fluorophore to the antipodal scaffold. However, it is not always a trivial task to obtain the opposite enantiomer, especially when they are of biochemical origin. In addition, the wavelength of CPL might be greatly changed. Consequently, it is desirable to develop a novel strategy for switching the CPL signs of chiral organic fluorophores without changing the chiral scaffold and modifying the fluorescent unit. In this relation, we have recently succeeded in controlling the CPL signs of chiral binaphthyl derivatives of the same axial chirality through manipulation of the dihedral angle of two naphthyl units by employing the internal steric hindrance and the external environmental factors.³ These results indicate that the CPL sign of a multi-fluorophore system is not inherent to the absolute configuration of the molecule but is manipulable or even switchable by altering the relative (geometrical) arrangement of the fluorophores.

In the present work, we report the unprecedented sign inversion of CPL from the regioisomeric fluorophores tethered to an identical chiral scaffold. To examine the effect of fluorophore geometry on the CPL behavior, we chose 1- and 2-naphthyls as fluorophores and enantiomeric *trans*-4,5-bis(hydroxymethyl)-1,3-dioxolane derived

from tartaric acid that is one of the most useful biochemical origin as a chiral scaffold: (4*R*,5*R*)- and (4*S*,5*S*)-2,2-dimethyl-*trans*-4,5-bis(di(1-naphthyl)hydroxymethyl)-1,3-dioxolane ((*R*)- and (*S*)-**1**) and (4*R*,5*R*)- and (4*S*,5*S*)-2,2-dimethyl-*trans*-4,5-bis(di(2-naphthyl)hydroxymethyl)-1,3-dioxolane ((*R*)- and (*S*)-**2**)⁴ (Scheme 1). This apparently trivial positional difference in naphthyl substituent led to the sign inversion in both CPL and CD spectra, the origin of which will be theoretically and experimentally elucidate from the conformational point of view.



Scheme 1 Organic fluorophores (*S*)-**1** and (*S*)-**2** that emit oppositely signed CPL, possessing four 1- or 2-naphthyl groups introduced to the same chiral scaffold derived from (*S,S*)-tartaric acid.

Fig. 1 (lower traces) compares the conventional (unpolarized) fluorescence spectra of **1** and **2** measured in chloroform. The fluorescence maxima (λ_{em}) appreciably differed between **1** and **2**, appearing at 344 and 336 nm, respectively, and the fluorescence quantum yields (Φ_F) were comparable at 0.02 for both **1** and **2**.

The CPL spectra of antipodal **1** and **2**, shown in Fig. 1 (upper traces), were reasonably mirror-imaged to each other (in shape and intensity) within the instrumental deviations. These CPL maxima (λ_{CPL}) for both (*S*)-**1** and (*S*)-**2** are not consistent in wavelength with the corresponding fluorescence maxima λ_{em} (344 and 336 nm) but redshifted to 418 and 381 nm, and the CPL bandwidths are not identical to each other. The significant shifts of up to 40 nm and the different bandwidths for (*S*)-**1** and (*S*)-**2** are rationalized by assuming existence of multiple conformers in the excited state, of which relaxed one(s), rather than the Frank-Condon state, emit stronger CPL.

More crucially, 1- and 2-naphthyls introduced to the same chiral scaffold, *i.e.* (*S*)-**1** and (*S*)-**2**, afforded the oppositely signed CPL spectra. For quantitative comparison, we employ the fluorescence

anisotropy factor (g_{em}), which is defined as $g_{em} = 2(I_L - I_R)/(I_L + I_R)$, where I_L and I_R denote the intensities of the left- and right-handed CPL observed upon excitation by unpolarized light. The absolute g_{em} values for λ_{CPL} were evaluated as $\sim 9.4 \times 10^{-3}$ at 410 nm and $\sim 3.9 \times 10^{-3}$ at 375 nm for **1** and **2**, respectively (Fig. 1). Both **1** and **2** exhibited fairly CPL behaviors, which are comparable in magnitude to those reported for other chiral organic fluorophores, the g_{em} value being in the range of 10^{-3} .² The smaller $|g_{em}|$ for **2** may be attributed at least in part to the higher conformational flexibility of less sterically demanding 2-naphthyls in **2** compared to 1-naphthyls in **1**. CPL profiles between 1.0 mM and 100 μ M are no much difference, but CPL profiles at 10 μ M are very noisy due to lower $|g_{em}|$ values.

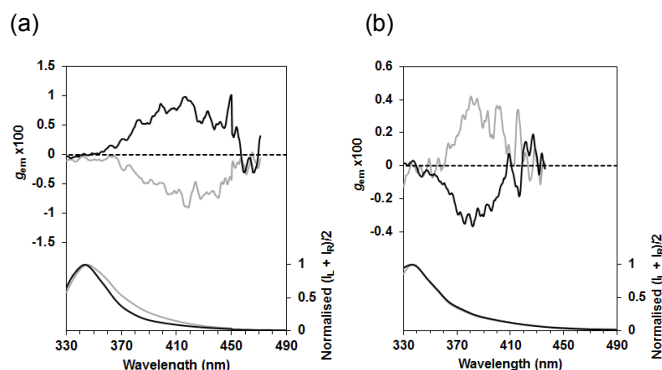


Fig. 1 CPL (upper traces) and fluorescence (lower traces) spectra of (a) **1**, and (b) **2** in chloroform (1.0 mM). The black and grey lines represent the (*S*)- and (*R*)-isomers, respectively.

This result unequivocally reveals that the CPL sign is not absolutely intrinsic to the chiral sense of the scaffold but is manipulable by altering the substitution position of the fluorophore tethered to the scaffold. To gain further insights into the origin of this unprecedented CPL sign inversion, we inspected the UV and CD spectra of **1** and **2** recorded at 100 μ M (Fig. 2) in the same solvent.

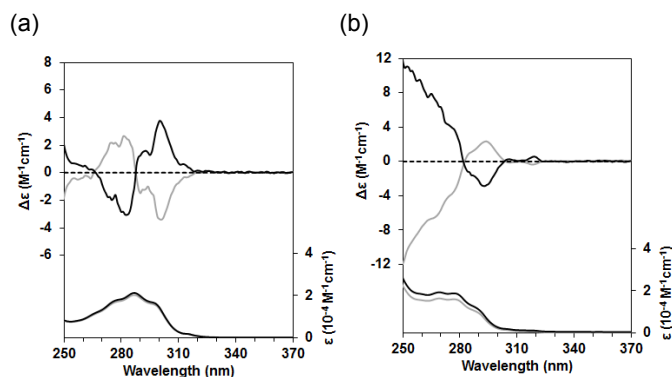


Fig. 2 CD (upper traces) and UV (lower traces) spectra of (a) **1**, and (b) **2** in chloroform (100 μ M). The black and grey lines represent the (*S*)- and (*R*)-isomers, respectively.

Both **1** and **2** exhibit the $\pi-\pi^*$ (1L_b and 1L_a) transitions of the naphthyl groups at 250-310 nm. Bisignate Cotton effects (CEs) of different magnitudes were observed for both **1** and **2** in this region, but the signs were inverted for the 1- and 2-naphthyl derivatives tethered to the same chiral scaffold (as was the case for CPL), affording the first positive/second negative CE pattern for (*S*)-**1** and the opposite for (*S*)-**2**. Kuhn's anisotropy factors for the first CE peaks were determined as $|g_{CD}| = |\Delta\epsilon/\epsilon| = \sim 2.4 \times 10^{-4}$ ($\lambda_{CD} = 301$ nm)

and $\sim 3.6 \times 10^{-4}$ ($\lambda_{CD} = 294$ nm) for **1** and **2**, respectively, which are one order of magnitude smaller than the corresponding $|g_{em}|$ values. Because the observed CPLs arise from the first excited singlet state ($S_1 \rightarrow S_0$), the reversal of the signs of the first CEs in CD ($S_0 \rightarrow S_1$) is responsible for the inverted signs of the CPL bands for (*S*)-**1** and (*S*)-**2**.

The sign-inverted CD and CPL spectra observed for **1** and **2** with the identical absolute configuration are most likely to originate from the difference in spatial arrangement of the four naphthyls. We therefore performed density functional theory (DFT) calculations to elucidate the origin of the CD/CPL sign inversion between **1** and **2**. The optimized structures of (*S*)-**1** and (*S*)-**2**, calculated by using the dispersion-corrected DFT method at the DFT-D3-TPSS/def2-TZVP level, are shown in Fig. 3.⁵ The equilibrium angles (θ) between the long axes of two germinal A/B and vicinal B/C, A/C, and A/D naphthyls of (*S*)-**1** are $+105.1^\circ$, $+92.4^\circ$, $+115.9^\circ$, and $+119.6^\circ$, respectively.

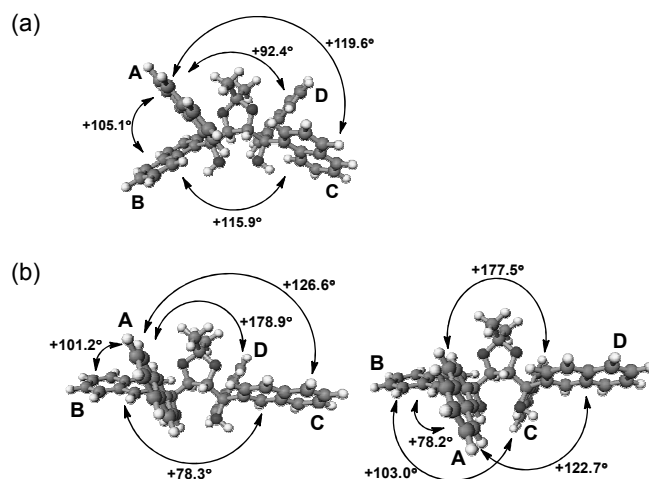


Fig. 3 Calculated structures of (a) (*S*)-**1**, and (b) two stable conformers of (*S*)-**2** obtained at the DFT-D3-TPSS/def2-TZVP level. The first conformer is more stable than the second by 0.4 kcal/mol. The angle is determined by the cross of long axis in each naphthalene ring.

The electronic excitations of (*S*)-**1** were theoretically examined to elucidate the origin of its first positive CE, and thus CPL. Recently, experimental CPL, PL, CD and UV-Vis spectra of a few chiral compounds using TD-DFT calculation with CAM-B3LYP and other several functionals have been successfully interpreted.⁶ Unfortunately, in this work, since (*S*)-/*R*)-**1** and (*S*)-/*R*)-**2** are more complex and larger molecular systems and have also four flexible naphthalene rings, it is difficult to calculate the optimized structures of **1** and **2** in the excited state. Therefore, first, the CD spectrum of (*S*)-**1** was directly calculated for the DFT-D3 optimized geometry by using the RI-CC2⁷ (curve *b*) and TD-DFT-CAM-B3LYP⁸ (curve *c*) methods (Fig. 4). First, the CD spectrum of (*S*)-**1** was directly calculated for the DFT-D3 optimized geometry by using the RI-CC2⁷ (curve *b*) and TD-DFT-CAM-B3LYP⁸ (curve *c*) methods (Fig. 4).

Regardless of the method employed, the first positive and second negative CEs were correctly reproduced with a slight overestimation in rotational strength, as usual. We further investigated the origin of CEs using the two-naphthalene and four-naphthalene models, in which two A/B, A/C, A/D, and B/C or four A/B/C/D naphthalenes were placed at the optimized geometry but the chiral scaffold was totally removed for simplicity purpose. The experimentally observed

first positive CE at ~ 300 nm was reproduced correctly only by the four-naphthalene model (curve *d*), while the summation of the CDs calculated for the four two-naphthalene models (curve *e*) failed to properly predict the sign of the first CE. This result reveals that the observed positive CPL/CD are not straightforwardly attributable to the excitonic coupling of two germinal/vicinal naphthalenes but originate from the more complicated coupling of the four chromophores.

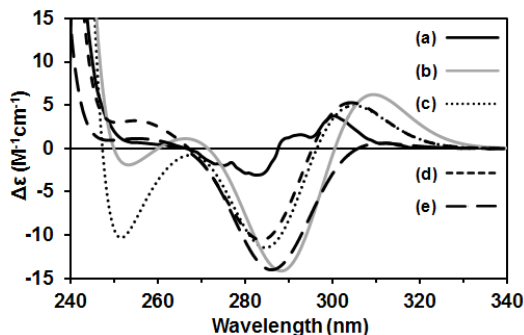


Fig. 4 Comparison of experimental and theoretical CD spectra of (*S*)-1. (a) experimental CD (100 μ M in chloroform), (b) theoretical CD obtained at the RI-CC2/TZVPP level, (c) theoretical CD obtained at the TD-DFT-CAM-B3LYP/TZVP level, (d) theoretical CD for the four-naphthalene model (A/B/C/D interactions were considered), and (e) the summation of the theoretical CDs of four pairs of the two-naphthalene models (incorporating A/B, A/C, A/D, and B/C naphthalenes). All theoretical CDs were scaled to one-third.

It is to note, however, that even the two-naphthalene model sufficiently reproduced the observed CD of (*S*)-1 at the main band (200–240 nm) (Fig. S1).

The CD spectra of (*S*)-2 was subjected to the same theoretical treatment employed for (*S*)-1. For (*S*)-2, two conformers were obtained by the calculation at the DFT-D3-TPSS/def-TZVP level, and their population was evaluated as 84:16 at 25 °C (at the SCS-MP2/TZVPP level)⁹ (Fig. 3b). The angle θ between the germinal or vicinal two naphthalenes significantly differ among the conformers, varying from +101.2° to +78.2°. Therefore, the simulated CD spectra for these conformers were mutually sign-inverted at both extrema (see Fig. S2). Thus, the theoretical CD spectra of (*S*)-2 were obtained by weight-averaging these spectra (Fig. 5).

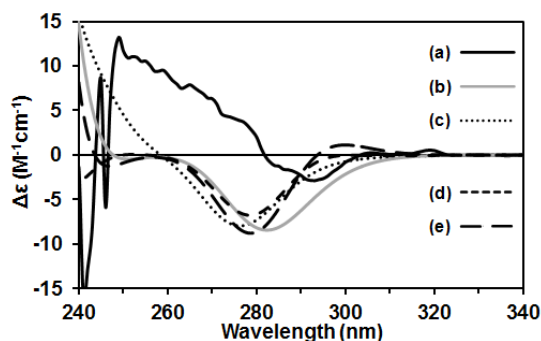


Fig. 5 Comparison of experimental and theoretical CD spectra of (*S*)-2. (a) experimental CD (100 μ M in chloroform), (b) theoretical CD obtained at the RI-CC2/TZVPP level, (c) theoretical CD obtained at the TD-DFT-CAM-B3LYP/TZVP level, (d) theoretical CD for the four-naphthalene model (A/B/C/D interactions were

considered), and (e) summation of the theoretical CDs of four pairs of the two-naphthalene models (incorporating A/B, A/C, A/D, and B/C naphthalenes). All theoretical CDs were obtained by averaging the two conformers assuming the Boltzmann distribution and scaled to one-third.

The first negative CE of (*S*)-2, which is opposite in sign to that of (*S*)-1, was correctly reproduced by these simulations (curves *b* and *c*) even after the considerable cancellation between the conformers. The theoretical rotational strengths were again overestimated compared to the observed CEs to some extent. It is noted that the sign of the CE at the main band in (*S*)-2 is the same as that for (*S*)-1 but the intensity is much reduced, which is in sharp contrast to the CE at the low energy band (Fig. S3). The theoretical investigations on these model systems revealed that the negative CE at the longest wavelength edge (~ 290 nm) mainly originates from the mixed interaction of the four naphthalenes, as was the case with (*S*)-1. Thus, the four-naphthalene model successfully reproduced this negative CE (curve *d*), while the two-naphthalene models failed to reproduce this band (curve *e*, see also Fig. S4). These results suggest that the sign-inversions of the first CD and CPL bands observed for (*S*)-1 and (*S*)-2 are attributable to the different spatial arrangement of four naphthalenes and the mixed coupling behavior of the relevant transitions.

Conclusions

We investigated the CPL and CD spectral behaviors of four germinal/vicinal naphthyl groups introduced to the identical chiral scaffold derived from enantiopure tartaric acid to find the unprecedented sign-inversion of both CPL and CD for 1- versus 2-naphthyl derivatives. The theoretical studies revealed that the sign inversion originates from the different spatial arrangements in the regioisomeric fluorophores and their complicated excitonic coupling interactions. From the practical point of view, the present finding provides us with an unconventional tool for switching the CPL (and CD) signs not by employing the antipodal scaffold but more conveniently by introducing regioisomeric fluorophores. This allows us to more freely design the organic CPL materials and manipulate their signs. Studies along this line are currently in progress.

This study was supported by a Grant-in-Aid for Scientific Research (Nos. 24550165, 25220802, 24655029, and 21245011) from MEXT/JSPS, MEXT-Supported Program for the Strategic Research Foundation at Private Universities, 2014-2018, the Mitsubishi Chemical Corporation Fund, the Sumitomo Foundation, the Shorai Foundation for Science and Technology, the Kurata Memorial Hitachi Science and Technology Foundation, the Tokuyama Science Foundation, and the KDDI Foundation.

Notes and references

^a Department of Applied Chemistry, Faculty of Science and Engineering, Kinki University, 3-4-1 Kowakae, Higashi-Osaka, Osaka 577-8502, Japan. E-mail: (Y.I.) y-imai@apch.kindai.ac.jp.

^b Department of Applied Chemistry, Osaka University, 2-1 Yamada-oka, Suita 565-0871, Japan. E-mail: (T.M.) tmori@chem.eng.osaka-u.ac.jp.

^c Graduate School of Materials Science, Nara Institute of Science and Technology, Takayama, Ikoma, Nara 630-0192, Japan. E-mail: (M.F.) fujikim@ms.naist.jp.

[†] Electronic Supplementary Information (ESI) available: Experimental details of measurements of PL, CD and CPL spectra, and theoretical calculations. Supporting figures and tables. See DOI: 10.1039/c000000x/.

- 1 (a) P. G. Coble, *Chem. Rev.*, 2007, **107**, 402; (b) T. P. I. Saragi, T. Spehr, A. Siebert, T. Fuhrmann-Lieker and J. Salbeck, *Chem. Rev.*, 2007, **107**, 1011; (c) S.-C. Lo and P. L. Burn, *Chem. Rev.*, 2007, **107**, 1097; (d) K. Walzer, B. Maennig, M. Pfeiffer and K. Leo, *Chem. Rev.*, 2007, **107**, 1233; (e) J. Grate, *Chem. Rev.*, 2008, **108**, 726; (f) F. Jakle, *Chem. Rev.*, 2010, **110**, 3985; (g) J. E. Kwon and S. Y. Park, *Adv. Mater.*, 2011, **23**, 3615; (h) C. Zhang, Y. S. Zhao and J. Yao, *New J. Chem.*, 2011, **35**, 973; (i) Lauren E. Kreno, Kirsty Leong, Omar K. Farha, Mark Allendorf, Richard P. Van Duyne, and Joseph T. Hupp, *Chem. Rev.*, 2012, **112**, 1105; and references cited therein.
- 2 (a) K. E. S. Phillips, T. J. Katz, S. Jockusch, A. J. Lovinger and N. J. Turro, *J. Am. Chem. Soc.*, 2001, **123**, 11899; (b) J. E. Field, G. Muller, J. P. Riehl and D. Venkataraman, *J. Am. Chem. Soc.*, 2003, **125**, 11808; (c) H. Maeda, Y. Bando, K. Shimomura, I. Yamada, M. Naito, K. Nobusawa, H. Tsumatori and T. Kawai, *J. Am. Chem. Soc.*, 2011, **133**, 9266; (d) R. Tempelaar, A. Stradomska, J. Knoester and F. C. Spano, *J. Phys. Chem., B*, 2011, **115**, 10592; (e) Y. Nakano and M. Fujiki, *Macromolecules*, 2011, **44**, 7511; (f) N. Nishiguchi, T. Kinuta, Y. Nakano, T. Harada, N. Tajima, T. Sato, M. Fujiki, R. Kuroda, Y. Matsubara and Y. Imai, *Chem. Asian J.*, 2011, **6**, 1092; (g) J. Liu, H. Su, L. Meng, Y. Zhao, C. Deng, J. C. Y. Ng, P. Lu, M. Faisal, J. W. Y. Lam, X. Huang, H. Wu, K. S. Wong and B. Z. Tang, *Chem Sci.*, 2012, **3**, 2737; (h) Y. Sawada, S. Furumi, A. Takai, M. Takeuchi, K. Noguchi and K. Tanaka, *J. Am. Chem. Soc.*, 2012, **134**, 4080; (i) H. Oyama, K. Nakano, T. Harada, R. Kuroda, M. Naito, K. Nobusawa and K. Nozaki, *Org. Lett.*, 2013, **15**, 2104; (j) J. Kumar, T. Nakashima, H. Tsumatori and T. Kawai, *J. Phys. Chem. Lett.*, 2014, **5**, 316; (k) T. Shiraki, Y. Tsuchiya, T. Noguchi, S.-i. Tamaru, N. Suzuki, M. Taguchi, M. Fujiki, and S. Shinkai, *Chem. Asian J.*, 2014, **9**, 218; (l) X. Jiang, X. Liu, Y. Jiang, Y. Quan, Y. Cheng and C. Zhu, *Macromol. Chem. Phys.*, 2014, **215**, 358; (m) Y. Morisaki, M. Gon, T. Sasamori, N. Tokitoh and Y. Chujo, *J. Am. Chem. Soc.*, 2014, **136**, 3350; (n) S. Abbate, G. Longhi, F. Lebon, E. Castiglioni, S. Superchi, L. Pisani, F. Fontana, F. Torricelli, T. Caronna, C. Villani, R. Sabia, M. Tommasini, A. Lucotti, D. Mendola, A. Mele and D. A. Lightner, *J. Phys. Chem. C*, 2014, **118**, 1682 and references cited therein.
- 3 (a) G. A. Hembury, V. V. Borovkov and Y. Inoue, *Chem. Rev.*, 2008, **108**, 1; (b) Y. Imai, K. Kawano, Y. Nakano, K. Kawaguchi, T. Harada, T. Sato, M. Fujiki, R. Kuroda and Y. Matsubara, *New J. Chem.*, 2008, **32**, 1110; (c) N. Nishiguchi, T. Kinuta, Y. Nakano, T. Harada, N. Tajima, T. Sato, M. Fujiki, R. Kuroda, Y. Matsubara and Y. Imai, *Chem. Asian J.*, 2011, **6**, 1092; (d) N. Nishiguchi, T. Kinuta, T. Sato, Y. Nakano, H. Tokutome, N. Tajima, M. Fujiki, R. Kuroda, Y. Matsubara and Y. Imai, *Chem. Asian J.*, 2012, **7**, 360; (e) T. Kinuta, N. Tajima, M. Fujiki, M. Miyazawa and Y. Imai, *Tetrahedron*, 2012, **68**, 4791; (f) T. Kimoto, N. Tajima, M. Fujiki and Y. Imai, *Chem. Asian J.*, 2012, **7**, 2836; (g) T. Amako, T. Kimoto, N. Tajima, M. Fujiki and Y. Imai, *RSC Advances*, 2013, **3**, 6939; (h) T. Kimoto, T. Amako, N. Tajima, R. Kuroda, M. Fujiki and Y. Imai, *Asian J. Org. Chem.*, 2013, **2**, 404.
- 4 H. Du, D. Zhao and K. Ding, *Chem. Eur. J.*, 2004, **10**, 5964.
- 5 (a) A. Schäfer, C. Huber and R. Ahlrichs, *J. Chem. Phys.*, 1994, **100**, 5829; (b) J. Tao, J. P. Perdew, V. N. Staroverov and G. E. Scuseria, *Phys. Rev. Lett.*, 2003, **91**, 146401/1; (c) S. Grimme and S. Ehrlich, *L. J. Goerigk, Comput. Chem.*, 2011, **32**, 1456; (d) S. Grimme, J. Antony, S. Ehrlich and H. Krieg, *J. Chem. Phys.*, 2010, **132**, 154104/1.
- 6 (a) B. Pritchard and J. Autschbach, *ChemPhysChem.*, 2010, **11**, 2409; (b) G. Longhi, E. Castiglioni, S. Abbate, F. Lebon and D. A. Lightner, *Chirality*, 2013, **25**, 589; (c) G. Longhi, S. Abbate, G. Mazzeo, E. Castiglioni, P. Mussini, T. Benincori, R. Martinazzo and F. Sannicolo, *J. Phys. Chem. C*, 2014, **118**, 16019.
- 7 (a) R. Christiansen, H. Koch and P. Jørgensen, *Chem. Phys. Lett.*, 1995, **243**, 409; (b) C. Hättig and F. Weigend, *J. Chem. Phys.*, 2000, **113**, 5154; (c) C. Hättig and A. Kohn, *J. Chem. Phys.*, 2002, **117**, 6939.
- 8 T. Yanai, D. Tew, N. Handy, *Chem. Phys. Lett.*, 2004, **393**, 51.
- 9 (a) S. Grimme, *J. Chem. Phys.*, 2003, **118**, 9095; (b) S. Grimme, L. Goerigk and R. F. Fink, *WIREs Comput Mol Sci.*, 2012, **2**, 886.

Graphical Abstract

